

# Linear space-variant optical processing of 1-D signals

J. W. Goodman, P. Kellman, and E. W. Hansen

In the past, most optical data processing systems have been restricted to performing linear space-invariant operations. However, a wide class of interesting data processing operations require linear space-variant filtering. Three methods for performing linear space-variant processing of 1-D inputs are described. Experimental results obtained with all three systems are presented, and their relative advantages and disadvantages are discussed.

## I. Introduction

In their traditional forms, optical data processing systems have been used primarily for the realization of linear, space-invariant operations. Such operations affect all parts of the input field identically and are mathematically describable in terms of convolutions.<sup>1</sup> However, many linear processing operations of interest are space-variant, i.e., they affect different parts of the input field in different fashions. Such operations must be described mathematically in terms of superposition integrals, rather than convolution integrals, and the usual Fourier theory of data processing no longer applies.

An important example of a linear space-variant operation that can be performed optically is Fourier transformation or spectral analysis. However, work on the use of optical systems for performing more general kinds of linear space-variant operations is not plentiful. Cutrona<sup>2</sup> recognized at an early date that coherent optical systems are capable of realizing a general superposition integral for 1-D inputs and showed one system which could be used for this purpose. More recently, Walkup and Hagler<sup>3,4</sup> have considered the use of thick holographic spatial filters for realizing space-variant operations. Methods for optically realizing space-variant operations by coordinate transformation processing, i.e., a sequence of geometrical distortions and linear space-invariant operations,<sup>5,6</sup> have been studied by Goodman.<sup>7,8</sup> Casasent and Psaltis<sup>9,10</sup> have used such an approach to perform Mellin transforms optically.

In this paper, we discuss several optical methods for performing space-variant linear operations on 1-D inputs, i.e., inputs that are functions of a single variable. In Sec. II we explain the mathematical basis of these methods and show how they can be implemented optically. In Sec. III, experimental results are presented for all the methods, and the experimental difficulties associated with each are discussed. Section IV contains some concluding remarks.

## II. Mathematical Representation and Optical Realization of 1-D Space-Variant Linear Operations

For a 1-D linear space-variant operation, the input  $f(x)$  and the output  $g(y)$  are related by a superposition integral<sup>1</sup>

$$g(y) = \int_{-\infty}^{\infty} h(y,x)f(x)dx, \quad (1)$$

where  $h(y,x)$  represents the response of the system at position  $y$  to a unit impulse applied at position  $x$ . This is perhaps the simplest way of relating the input and output. For a space-invariant operation,  $h(y,x)$  depends only on the difference of coordinates ( $y - x$ ), and Eq. (1) becomes a convolution integral.

To illustrate with some specific space-variant operations of interest, we mention the following:

(1) Geometrical distortions (or coordinate transformations):

$$g(y) = f[z(y)] = \int_{-\infty}^{\infty} \delta[z(y) - x]f(x)dx, \\ h(y,x) = \delta[z(y) - x]; \quad (2)$$

(2) Mellin transform<sup>11</sup>:

$$g(y) = \int_0^{\infty} x^{y-1}f(x)dx, \\ h(y,x) = x^{y-1}U(x), \quad (3)$$

where

The authors are with Department of Electrical Engineering, Stanford University, Stanford, California 94305.

Received 2 September 1976.

$$U(x) = \begin{cases} 1 & x > 0; \\ 1/2 & x = 0; \\ 0 & x < 0 \end{cases}$$

(3) Inverse Abel transform<sup>11</sup>:

$$g(y) = -\frac{1}{\pi} \int_{|y|}^{\infty} \frac{f'(x) dx}{(x^2 - y^2)^{1/2}}$$

$$h(y, x) = -\frac{1}{\pi(x^2 - y^2)^{1/2}} U(x - |y|) \frac{d}{dx} [ \quad ], \quad (4)$$

where  $d/(dx)[ \quad ]$  is a differentiation operator which operates only on the input  $f(x)$ .

Many other examples could be mentioned, but for brevity we terminate here.

To realize optically the operation described by Eq. (1), the optical system shown in Fig. 1 can be used. This system is essentially equivalent to that discussed by Cutrona.<sup>2</sup> The cylindrical lens  $L_1$  illuminates the input function through a horizontal slit in plane  $P_1$ . Lens combination  $L_2$  serves to image in the  $x$  direction while it Fourier transforms in the  $y$  direction. The Fourier transformation simply spreads the image of the input vertically without affecting its horizontal structure. In plane  $P_2$  we place a transparency with amplitude transmittance  $t(x, y) = h(y, x)$ . Lens combination  $L_3$  images in the  $y$  direction and Fourier transforms in the  $x$  direction.<sup>12</sup> The output is obtained through a vertical slit coinciding with the  $y$  axis in plane  $P_3$ . Along this axis the Fourier transform becomes a simple integration with respect to  $x$ , as required by Eq. (1). While we have explained the operation of the system under the assumption that the light is completely coherent, the method will also work when the illumination is spatially incoherent in the  $x$  direction, but full coherence in the  $y$  direction is desirable from the point of view of efficient light usage.

A second possible approach to realizing a space-variant filter can be found by applying Parseval's theorem<sup>13</sup> to the right-hand side of Eq. (1). Defining

$$\hat{f}(\nu_X) = \int_{-\infty}^{\infty} f(x) \exp(-i2\pi\nu_X x) dx,$$

$$\hat{h}(\nu_Y, \nu_X) = \int_{-\infty}^{\infty} h(y, x) \exp(-i2\pi\nu_X x) dx, \quad (5)$$

we have

$$g(y) = \int_{-\infty}^{\infty} \hat{h}(\nu_Y, -\nu_X) \hat{f}(\nu_X) d\nu_X. \quad (6)$$

This mathematical form suggests the optical realization shown in Fig. 2. Again the line-function input  $f(x)$  is illuminated by means of a cylindrical lens  $L_1$ . Lens  $L_2$  is in this case a spherical lens, and planes  $P_1$  and  $P_2$  coincide with its front and back focal planes, respectively. In the  $x$  direction, the input function is Fourier transformed, while the effect of the lens in the vertical direction is simply to spread this spectrum vertically by virtue of the Fourier transformation of the narrow input slit. In plane  $P_2$  we insert a mask with amplitude transmittance proportional to  $\hat{h}(\nu_Y, -\nu_X)$ . Lens  $L_3$  is a combination of cylindrical and spherical elements such

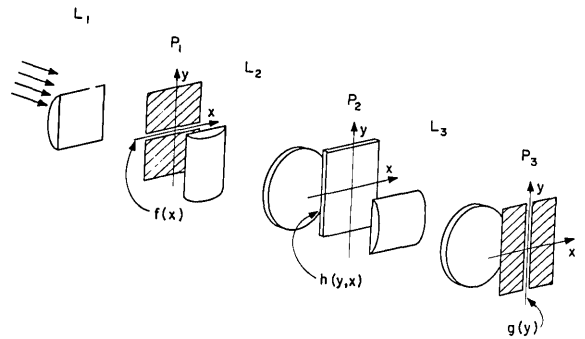


Fig. 1. Filtering system which uses two spherical-cylindrical lens combinations.

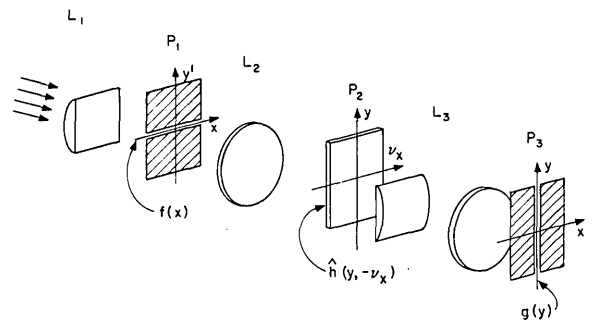


Fig. 2. Filtering system which uses one spherical-cylindrical lens combination and one purely spherical lens.

that plane  $P_2$  is imaged onto  $P_3$  in the  $y$  direction, but Fourier transformed in the  $x$  direction. A vertical output slit along the  $y$  axis then passes the desired integral.

Note that the transparency with complex amplitude transmittance  $\hat{h}(\nu_Y, -\nu_X)$  must in general be a hologram. This hologram can be computer-generated or optically generated, as discussed in more detail in Sec. III. If the hologram has a carrier frequency in the  $\nu_X$  direction, the output slit must be displaced horizontally to coincide with the position of the carrier frequency in the output plane.

A third and final approach to the realization of the superposition integral can be found by Fourier transforming Eq. (6) with respect to  $y$ , giving

$$\hat{g}(\nu_Y) = \int_{-\infty}^{\infty} \hat{h}(\nu_Y, -\nu_X) \hat{f}(\nu_X) d\nu_X, \quad (7)$$

where

$$\hat{g}(\nu_Y) = \int_{-\infty}^{\infty} g(y) \exp(-i2\pi\nu_Y y) dy,$$

$$\hat{h}(\nu_Y, -\nu_X) = \int_{-\infty}^{\infty} \int_{-\infty}^{\infty} h(y, x) \exp[-i2\pi(\nu_Y y - \nu_X x)] dy dx. \quad (8)$$

Applying an inverse Fourier transform to Eq. (7), we find

$$g(y) = \int_{-\infty}^{\infty} \int_{-\infty}^{\infty} \hat{h}(\nu_Y, -\nu_X) \hat{f}(\nu_X) \exp(i2\pi\nu_Y y) d\nu_X d\nu_Y. \quad (9)$$

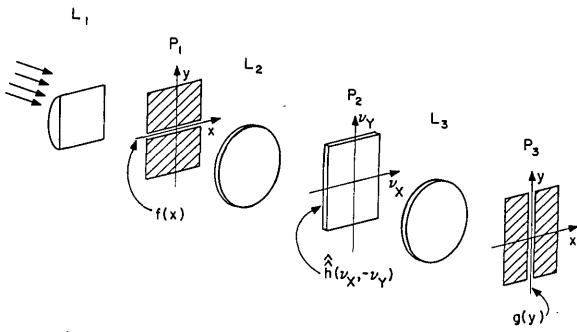
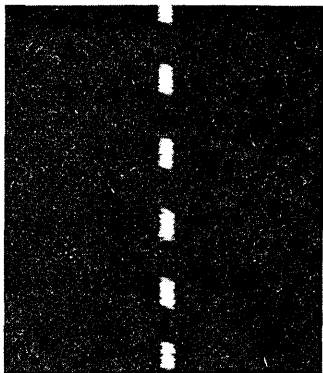
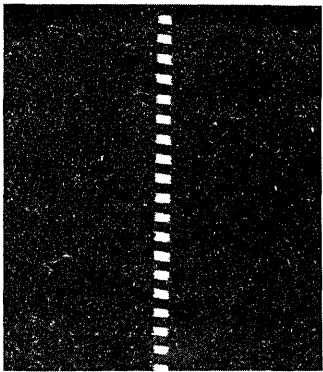


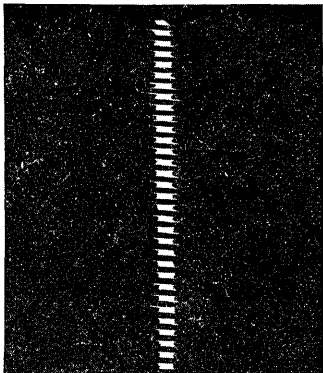
Fig. 3. Filtering system which uses two purely spherical lenses.



(a)



(b)



(c)

Fig. 4. Variable magnifier realized with the system of Fig. 1: (a) slit angle 10°; (b) slit angle 30°; (c) slit angle 45° (output slit removed).

The operations indicated in Eq. (9) can be implemented optically by the system shown in Fig. 3. Again the input function is illuminated by the cylindrical lens  $L_1$ . Lens  $L_2$  is spherical, and Fourier transforms the input function in both directions. The effect of the vertical transformation of the narrow input slit is simply to spread out the horizontal transform in the vertical direction. In plane  $P_2$  we place a mask with complex amplitude transmittance  $\hat{h}(\nu_Y, -\nu_X)$ . Lens  $L_3$  is spherical and again performs a 2-D Fourier transformation. A vertical output slit along the  $y$  axis (or displaced horizontally if  $\hat{h}$  is realized as a carrier-frequency hologram) achieves a simple integration in the  $\nu_X$  direction and a Fourier transformation in the  $\nu_Y$  direction, as required by Eq. (9).

In summary, we have described three different but related ways to optically realize the superposition integral of Eq. (1). In the next section we show some experimental results obtained with each type of system and discuss some advantages and disadvantages of each.

### III. Experimental Results

All three systems described above have been realized optically and have been used to perform very simple space-variant operations. In the following we describe the results and indicate some of the advantages and disadvantages associated with each approach.

The system of Fig. 1 has been used to realize two different space-variant operations. The simplest is that of a variable magnifier, which has an impulse response described by

$$h(y,x) = \delta(y - Mx). \quad (10)$$

Thus the mask  $h(y,x)$  in plane  $P_2$  consists of a simple straight slit, passing through the origin and having slope  $M$ , which is the magnification desired. The input function  $f(x)$  in this experiment was a square wave provided by a 20-lines/cm Ronchi ruling. Figures 4(a), 4(b), and 4(c) show the outputs obtained in plane  $P_3$  without the vertical output slit inserted and with three different slit angles in plane  $P_2$ . The width of this slit was 80  $\mu\text{m}$  in these three cases.

A second experiment was performed with the system of Fig. 1. In this case the input consisted of two small openings in an opaque mask,

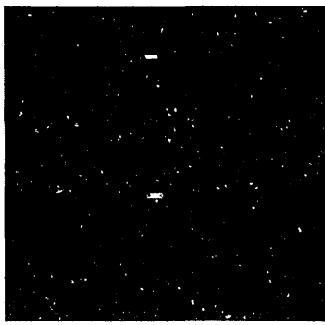
$$f(x) = \delta(x - x_1) + \delta(x - x_2) \quad (11)$$

as shown in Fig. 5(a). The transparency  $h(y,x)$  was a transparent pie-shaped slit, centered on the origin, mathematically described by

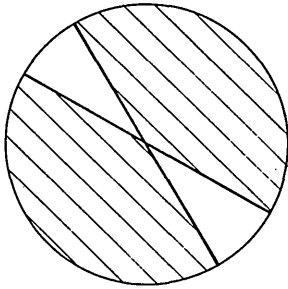
$$h(y,x) = \text{rect} \left( \frac{y-x}{bx} \right), \quad (12)$$

where  $b$  is a constant, as shown in Fig. 5(b). The output, shown in Fig. 5(c), consists of two pulses blurred by different amounts, depending on their location along the  $y$  axis.

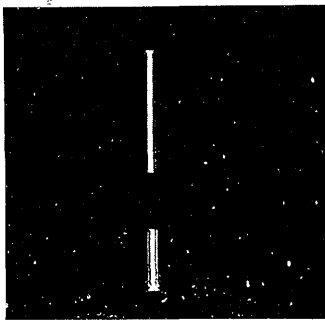
The chief advantages of the system of Fig. 1 are its conceptual simplicity and the ease with which the required mask  $h(y,x)$  can usually be specified. In addition, in many cases of interest this mask is relatively



(a)



(b)



(c)

Fig. 5. Variable blur realized with the system of Fig. 1: (a) input function; (b) mask in plane  $P_2$ ; (c) output (output slit removed).

easy to make. However, the system also has at least two disadvantages. Most important, the lenses  $L_2$  and  $L_3$  are spherical-cylindrical combinations, and it is difficult to obtain high quality cylindrical components. (Note that the cylindrical lens  $L_1$  is common to all three systems, but need not be of high quality.) As a second disadvantage, we note that any impulse response containing a derivative operator [such as Eq. (4)] is difficult to realize by this method.

Turning now to the system of Fig. 2, we describe another simple experiment. In this case the goal was to perform the geometrical transformation  $g(y) = f(\sqrt{y})$ . A mask having two transparent curved slits was prepared, as shown in Fig. 6(a). The transmittance of this mask was approximately

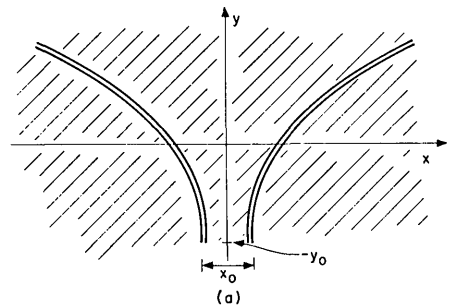
$$t(x,y) = \delta \left[ x - \frac{x_0}{2} - (y + y_0)^{1/2} \right] + \delta \left[ x + \frac{x_0}{2} + (y + y_0)^{1/2} \right] \quad (13)$$

for  $y \geq -y_0$ . This mask was inserted in the system of Fig. 6(b) which Fourier transforms horizontally and images vertically. The resulting recording may be regarded as a hologram and has an amplitude transmittance of the form

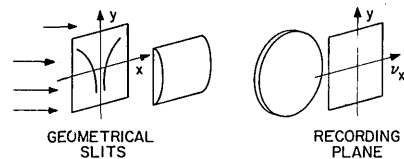
$$t(\nu_X, y) = k_1 + k_2 \cos[\pi\nu_X x_0 + 2\pi\nu_X (y + y_0)^{1/2}], \quad (14)$$

where  $k_1$  and  $k_2$  are constants.

The transparency with transmittance described by Eq. (14) is inserted in plane  $P_2$  of Fig. 2. A Ronchi ruling (20 lines/cm) is again placed in the input plane  $P_2$ . At the output of the system we find the image shown in Fig. 7 (output slit removed). This image consists of a zero-order image of the input Ronchi ruling,



(a)



(b)

Fig. 6. Recording of the required filter: (a) transparent slits; (b) recording geometry.

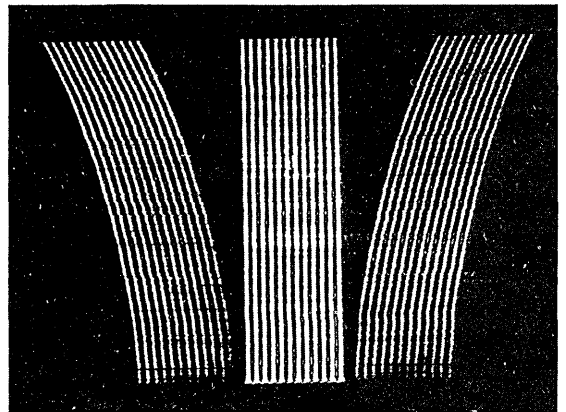
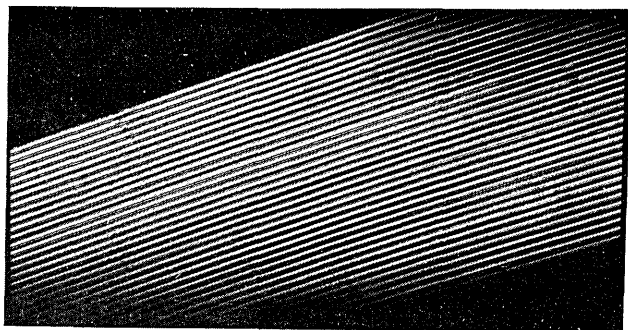


Fig. 7. Output of the system of Fig. 2, with output slit removed, and using the holographic filter generated as in Fig. 6.

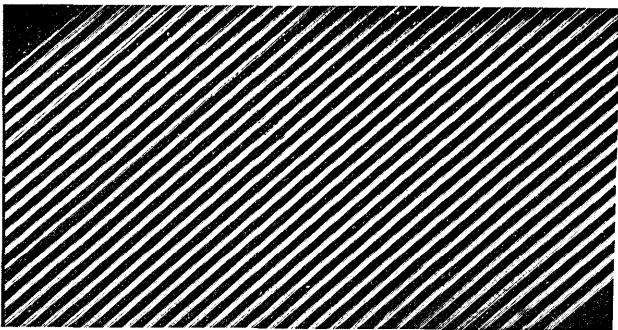
spread vertically, plus two first-order images resembling bent Ronchi rulings. A vertical output slit appropriately placed in one of the first-order images yields the desired 1-D output.

The chief advantages of this system over the system of Fig. 1 are that it requires only one spherical-cylindrical lens combination and that it has high light efficiency for operations that are close to geometrical distortions. The chief disadvantage of the system is the necessity to generate a holographic filter.

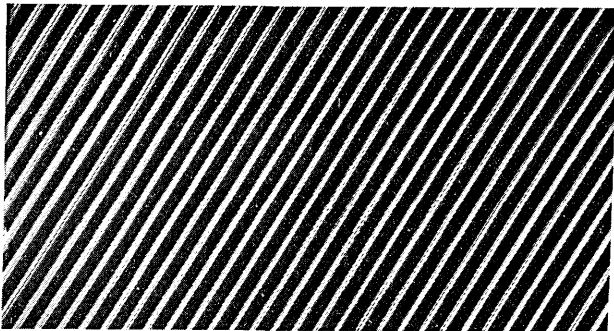
Turning finally to the system of Fig. 3, we consider



(a)



(b)



(c)

Fig. 8. Output of the system of Fig. 3 operated as a variable magnifier (output slit removed): (a) slit angle 20°; (b) slit angle 40°; (c) slit angle 60°.

the realization of a variable magnifier using this approach. Knowing that the variable magnifier has an impulse response described by Eq. (10), we apply the 2-D transform of Eq. (8) to find the required mask to be placed in plane  $P_2$  of Fig. 3. The result is

$$\hat{h}(\nu_Y, -\nu_X) = \delta(\nu_X - M\nu_Y). \quad (15)$$

Thus the required mask is again a simple slit, but with a different orientation than the corresponding slit required for the system of Fig. 1. Figure 8 shows the output of the system for three different slit angles, or equivalently three different magnifications. In all cases the output slit has been removed.

The advantage of this final system is the fact that it requires only spherical optics (aside from the noncritical cylindrical lens  $L_1$ ). A disadvantage is that, at least for the variable magnifier realized here, the light efficiency was less than that of the systems of Figs. 1 and 2. The usable output field (space-bandwidth product) was limited by the finite width of the filter slit. In addition, in the case of a more general filtering operation, it is necessary to make a Fourier transform hologram of the desired impulse response rather than using that impulse response directly.

#### IV. Concluding Remarks

We have described three different methods for performing space-variant filtering operations on 1-D inputs. The first method (Fig. 1) is a modified version of the system described by Cutrona<sup>2</sup> more than 10 years ago. Both the first and second methods (Figs. 1 and 2) are related to techniques described by Rhodes and Florence<sup>14</sup> for frequency-variant filtering. The third method (Fig. 3) appears to be unrelated to any previous work, but is a logical extension of the first two methods.

An entirely different method for performing coordinate transformations in two dimensions has been described by Bryngdahl.<sup>15</sup> While this method is more general in the sense that it is not limited to 1-D inputs, it suffers from a severe limitation on the space bandwidth product of the input to be processed. This limitation arises from a mathematical approximation which is valid provided the spatial frequency content of the input is considerably smaller than the highest spatial frequency contained in the computer-generated hologram that performs the coordinate transformation. No such limitation is present for the techniques described here.

Finally, it should be mentioned that an ideal space-variant filtering technique, capable of filtering 2-D functions with large space-bandwidth products, is not yet known.

This work was sponsored in part by the Office of Naval Research and in part by the National Science Foundation.

## References

1. J. W. Goodman, *Introduction to Fourier Optics* (McGraw-Hill, New York 1968), Sec. 2-2.
  2. L. J. Cutrona, "Recent Developments in Coherent Optical Technology," in *Optical and Electro-Optical Information Processing*, J. T. Tippett, D. A. Berkowitz, L. C. Clapp, C. J. Koester, and A. Vanderburgh, Jr., Eds. (MIT Press, Cambridge, 1965), Chap. 6.
  3. J. F. Walkup and M. O. Hagler, "Volume Hologram Representations of Space-Variant Optical Systems," in *Proceedings 1975 Electro-Optical System Design Conference* (Industrial and Scientific Conference Management, Inc., Chicago, 1975), pp. 38-41.
  4. L. M. Deen, J. F. Walkup, and M. O. Hagler, *Appl. Opt.* **14**, 2438 (1975).
  5. G. M. Robbins and T. S. Huang, *Proc. IEEE* **60**, 862 (1972).
  6. A. A. Sawchuk, *Proc. IEEE* **60**, 854 (1972).
  7. J. W. Goodman, "Operations Achievable with Coherent Optical Data Processing," in *Proceedings 1975 Electro-Optical System Design Conference* (Industrial and Scientific Conference Management, Inc., Chicago, 1975), pp. 1-8.
  8. J. W. Goodman, *Proc. IEEE* **65**, 29 (1977).
  9. D. Casasent and D. Psaltis, "Mellen Transforms in Optical Data Processing," in *Proceedings 1975 Electro-Optical System, Design Conference* (Industrial and Scientific Conference Management, Inc., Chicago, 1975), pp. 38-41.
  10. D. Casasent and D. Psaltis, *Opt. Eng.* **15**, 258 (1976).
  11. R. Bracewell, *The Fourier Transform and its Applications* (McGraw-Hill, New York, 1965).
  12. The quadratic phase factor existing in the y direction in plane  $P_3$  is of no consequence, since  $L_3$  images in this direction.
  13. A. Papoulis, *The Fourier Integral and its Applications* (McGraw-Hill, New York, 1962), p. 27.
  14. W. T. Rhodes and J. M. Florence, *Appl. Opt.* **15**, 3073 (1976).
  15. O. Bryngdahl, *J. Opt. Soc. Am.* **64**, 1092 (1974).
- 

### Digital Techniques in Spectral Analysis, Estimation, and Filtering: A Computer Workshop March 7-11, 1977

Covers practical computer techniques for signal processing, including fast Fourier Transforms, digital filter design, spectral analysis, detection, estimation, and Kalman filtering. Applications to diverse fields including speech and EEG signals. Participants will solve problems on a CDC 6500 computer.

### Image Processing and Pattern Recognition March 14-18, 1977

Covers principles and techniques of image coding, restoration and enhancement, segmentation, feature extraction, recognition, syntactical analysis. Applications to diverse areas, especially remote sensing and biomedicine.

For further details, contact:

Mark Ocker  
Conference Division  
Stewart Center  
Purdue University  
West Lafayette, Indiana 47907  
Telephone Number (317) 749-2533